第37卷第4期
2021年4月

无 机 化 学 学 报
CHINESE JOURNAL OF INORGANIC CHEMISTRY

Vol.37 No.4
592-600

含羟基基团取代的氮氧自由基构筑的三个双核稀土化合物的结构及磁性表征

梅雪兰*,[1] 郭简妮[2] 杜敏杰[3] 杨培培*,[4] 李 倩[1] 李宗群[1] 瞿安荣[1]

([1]蚌埠学院材料与化学工程学院,蚌埠 233030)

([2]南开大学化学学院化学系,先进能源材料化学重点实验室,天津 300071)

([3]南京军代局驻蚌埠地区军代室,蚌埠 233030)

([4]淮北师范大学化学与材料科学学院,淮北 235000)

摘要: 以三氟乙酰丙酮(tfac)为共配体的稀土配合物分别与5-溴-2-羟基苯取代的自由基配体和5-硝基-2-羟基苯取代的自由基配体进行反应,合成3个稀土-自由基配合物[$Ln_2(tfac)_4$(NIT-5Br-2PhO)$_2$](Ln=Gd (**1**), Dy (**2**))和[$Dy_2(tfac)_4$(NIT-5NO_2-2PhO)$_2$] (**3**)(NIT-5Br-2PhOH=2-(2′-hydroxy-5′-bromophenyl)-4,4,5,5-tetramethylimidazoline-1-oxyl-3-oxide, NIT-5NO_2-2PhOH=2-(2′-hydroxy-5′-nitrophenyl)-4,4,5,5-tetra-methylimidazoline-1-oxyl-3-oxide)。单晶结构分析表明这3个化合物中的稀土离子均通过自由基配体上的羟基氧基团连接为双核的结构。配合物**1**的直流磁化率表征揭示了Gd(Ⅲ)离子间的反铁磁耦合对其磁行为起主要作用。

关键词: 稀土配合物; 氮氧自由基; 双核结构; 磁行为

中图分类号: O614.33$^+$9; O614.342 **文献标识码:** A **文章编号:** 1001-4861(2021)04-0592-09

DOI: 10.11862/CJIC.2021.073

Three Binuclear Lanthanide Complexes Constructed from Nitronyl Nitroxide Radical Ligands Containing Phenol Groups: Structure and Magnetic Properties

MEI Xue-Lan*,[1] GUO Jian-Ni[2] DU Min-Jie[3] YANG Pei-Pei*,[4] LI Qian[1] LI Zong-Qun[1] QU An-Rong[1]

([1]*College of Materials Science and Chemical Engineering, Bengbu University, Bengbu, Anhui* 233030, *China*)

([2]*Department of Chemistry, Key Laboratory of Advanced Energy Materials Chemistry, College of Chemistry, Nankai University, Tianjin* 300071, *China*)

([3]*Military Representative Bureau of Nanjing of the PLA Army, Bengbu, Anhui* 233030, *China*)

([4]*College of Chemistry and Materials Science, Huaibei Normal University, Huaibei, Anhui* 235000, *China*)

Abstract: The nitronyl nitroxide radicals NIT-5Br-2PhOH (2-(2′-hydroxy-5′-bromophenyl)-4,4,5,5-tetramethylimidazoline-1-oxyl-3-oxide) and NIT-5NO_2-2PhOH (2-(2′-hydroxy-5′-nitrophenyl)-4,4,5,5-tetramethylimidazoline-1-oxyl-3-oxide) were selected as ligands to react with Ln(tfac)$_3$·2H_2O (tfac=trifluoroacetylacetonate) to produce three new lanthanide-radical complexes [Ln(tfac)$_2$(NIT-5Br-2PhO)]$_2$ (Ln=Gd (**1**), Dy (**2**)) and [Dy(tfac)$_2$(NIT-5NO_2-2PhO)]$_2$ (**3**). Single crystal X-ray crystallographic analysis reveals that all three complexes possess binuclear structure in which two lanthanide ions are connected through the hydroxy groups of the radicals. DC magnetic susceptibilities of Gd complex reveal that the antiferromagnetic coupling between the Gd(Ⅲ) centers plays a major role for the magnetic behavior. CCDC: 1981623, **1**; 1981622, **2**; 2021836, **3**.

Keywords: lanthanide complexes; nitronyl nitroxide radical; binuclear structure; magnetic behavior

收稿日期:2020-08-15。收修改稿日期:2020-12-30。

安徽高校自然科学基金(No.KJ2017A571)、蚌埠学院自然科学基金(No.2017ZR01zd)、蚌埠学院产学研项目(精密塑料零件成型工艺参数优化)和大学生创新创业项目(No.201811305146)资助。

*通信联系人。E-mail:daluhuashu@qq.com,394117773@qq.com

0 Introduction

Single-molecule magnets (SMMs) have become one of the most popular research in molecular area for their potential applications in the molecular spintronics, quantum computing, and high density magnetic storage. Since the first Ln (Ⅲ)-radical based SMM $[Dy(hfac)_3NITpPy]_2$[1] was discovered, rare earth-radical complexes have attracted tremendous attention. The rather large and anisotropic magnetic moments of lanthanide (Ⅲ) ions and effective magnetic exchange between the radical and metal ion make this approach very appealing for the preparation of magnetic materials[2-7]. Up to now, various 4*f*-radical systems revealing appealing magnetic properties have been achieved, *e.g.* mononuclear 4*f*-radical[8-15] and 4*f*-biradical complexes[16-19], dinuclear 4*f*-radical[20-29] and 4*f*-biradical dimmers[30], polynuclear 4*f*-radical complexes[31-34]. Furthermore, magnetic characterization indicates that some of these 4*f*-radical complexes have the SMM behaviors. A perusal of the literature displays that the nitronyl nitroxide radicals (NITR) have more advantages to design magnetic materials comparing to others for their relative stability and chemically modifying easily to obtain derivatives with substituents containing donor atoms[35], and so on. Based on these advantages, we can also find that using the nitronyl nitroxide radicals including functionalized nitronyl nitroxides with 4*f* ions is an excellent strategy to build magnetic complexes. Actually, the strategy has been responsible for many developments in single-molecule magnetism, obtaining a lot of 4*f*-NITR SMMs with different structures and remarkable magnetic properties, such as ring-like 4*f*-NITR SMMs[36-37]. But still more problems need to be solved for increasing magnetic exchange interactions and the rational design of spin topologies with interesting magnetic properties.

On account of the above consideration, to investigate the magnetic properties and structures of 4*f*-NITR complexes further, we focused on nitronyl nitroxide radicals with phenol group which could act as a commendable candidate to coordinate with lanthanide ions via chelating and bridging mode, leading to complexes with appealing structures. Accordingly, the radicals NIT-5Br-2PhOH and NIT-$5NO_2$-2PhOH (NIT-5Br-2PhOH=2-(2′-hydroxy-5′-bromophenyl)-4,4,5,5-tetramethylimidazoline-1-oxyl-3-oxide, NIT-$5NO_2$-2PhOH=2-(2′-hydroxy-5′-nitrophenyl)-4,4,5,5-tetramethylimidazoline-1-oxyl-3-oxide, Scheme 1) were employed to construct 2*p*-4*f* complexes, in which both the radicals have the same parent structures but different substituents, for probing the effects of ligand field perturbation on the properties of complexes. Meanwhile, we chose trifluoroacetylacetonate (tfac) as the coligand to strengthen Lewis acidity necessary for the coordination of the radicals to the 4*f* ions. We synthesized three new Ln-radical-based complexes, $[Ln_2(tfac)_4(NIT\text{-}5Br\text{-}2PhO)_2]$ (Ln=Gd (**1**), Dy (**2**)) and $[Dy_2(tfac)_4(NIT\text{-}5NO_2\text{-}2PhO)_2]$ (**3**), whose crystal structures and magnetic properties were also investigated.

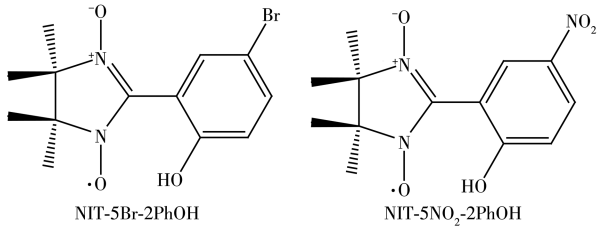

Scheme 1 Nitronyl nitroxide radicals NIT-5Br-2PhOH and NIT-$5NO_2$-2PhOH

1 Experimental

1.1 Materials and physical measurements

All solvents and chemicals used in the syntheses were reagent-grade without further purification. Syntheses of $Ln(tfac)_3\cdot 2H_2O$ (Ln=Gd, Dy) have been performed according to the method in the literature[38]. The radical ligands NIT-5Br-2PhOH and NIT-$5NO_2$-2PhOH were prepared by the reported methods[39-41]. Elemental analyses for C, H and N were carried out at the Institute of Elemental Organic Chemistry, Nankai University. IR spectra were recorded in a range of 400~4 000 cm^{-1} on a Bruker Tensor 27 FT-IR spectrometer with samples as KBr disks. Magnetic measurements were performed on a SQUID MPMS XL-7 magnetometer. Meanwhile, diamagnetic corrections were made with Pascal′s constants for all of the constituent atoms.

1.2 Synthesis of the complexes

1.2.1 Preparation of $[Gd_2(tfac)_4(NIT\text{-}5Br\text{-}2PhO)_2]$ (**1**)

$Gd(tfac)_3 \cdot 2H_2O$ (0.131 g, 0.2 mmol) was dissolved in 30 mL dry boiling heptane, and the solution remained refluxing for 3 h and then was cooled down to 70 ℃. Then a solution of NIT-5Br-2PhOH (0.066 g, 0.2 mmol) in 5 mL of CH_2Cl_2 was added. The resulting solution was stirred for 10 min at 70 ℃, then cooled to room temperature. Whereafter, the mixture was filtrated, and the filtrate was kept in the dark and concentrated slowly by evaporation at room temperature. Aubergine crystals were obtained after two days. Yield: 77%. Elemental analysis Calcd. for $C_{46}H_{46}N_4O_{14}F_{12}Br_2Gd_2$(%): C, 34.94; H, 2.93; N, 3.54. Found(%): C, 34.95; H, 3.22; N, 3.62. IR (KBr, cm^{-1}): 3 445(w), 1 630(s), 1 531(m), 1 486(m), 1 368(s), 1 224(s), 1 187(m), 1 132(s), 857(w), 826(w), 775(w), 725(w), 676(w), 626(w), 561(w).

1.2.2 Preparation of $[Dy_2(tfac)_4(NIT\text{-}5Br\text{-}2PhO)_2]$ (**2**)

The process was same as that for complex **1** except that $Dy(tfac)_3 \cdot 2H_2O$ (0.132 g, 0.2 mmol) was used in place of $Gd(tfac)_3 \cdot 2H_2O$ (0.131 g, 0.2 mmol). Yield: 72%. Elemental analysis Calcd. for $C_{46}H_{46}N_4O_{14}F_{12}Br_2Dy_2$(%): C, 34.71; H, 2.91; N, 3.50. Found(%): C, 34.75; H, 3.10; N, 3.63. IR (KBr, cm^{-1}): 3 447(w), 1 630(s), 1 532(m), 1 486(m), 1 368(s), 1 224(s), 1 186(m), 1 132(s), 857(w), 826(w), 775(w), 728(w), 677(w), 626(w), 563(w).

1.2.3 Preparation of $[Dy_2(tfac)_4(NIT\text{-}5NO_2\text{-}2PhO)_2]$ (**3**)

A same procedure as that for complex **2** was followed to prepare complex 3, except that NIT-5Br-2PhOH was replaced by $NIT\text{-}5NO_2\text{-}2PhOH$ (0.059 g, 0.2 mmol). Yield: 72%. Elemental analysis Calcd. for $C_{46}H_{46}F_{12}N_6O_{18}Dy_2$(%): C, 36.26; H, 3.04; N, 5.51. Found(%): C, 36.63; H, 3.32; N, 5.90. IR (KBr, cm^{-1}): 1 620(s), 1 577(m), 1 345(m), 1 291(m), 1 161(s), 1 067(s), 948(s), 861(s), 547(s), 517(s).

1.3 X-ray crystallography

X-ray single-crystal diffractions of complexes **1~3** were performed on a Rigaku mercury CCD diffractometer with graphite monochromated Mo $K\alpha$ radiation (λ = 0.071 073 nm) at 113(2) K. In each case, absorption corrections were applied. The structures were solved by direct methods and refined with full-matrix least-squares technique using the SHELXS-97 and SHELXL-97 programs[42-43]. All non-hydrogen atoms were refined anisotropically while hydrogen atoms were added theoretically and refined isotropically using a riding mode. Some disordered fragments of structures were found for some carbon, oxygen and fluorine atoms of tfac. The restraints by ISOR, DFIX, DELU and SIMU were applied to three complexes to keep the disordered molecules reasonable[44]. More specifically, for complex **1**, the F1, F2, F3 atoms of one tfac ligand were disordered over two orientations and refined with site-occupation factors of 0.501∶0.499; for complex **2**, the F4, F5, F6 atoms of the disordered coordinated tfac ligand were divided into two parts with occupancies tatio of 0.500∶0.500; and for complex **3**, the C16, C17, C21, C22, C23, O6 and F4 atoms in the two tfac ligands were positionally disordered and each disorder components were refined as half-occupied. Meanwhile, the bond lengths of C1—F1′, C1—F2′, C1—F3′, C5—F1, C5—F2, C5—F3 (complex **1**), C6—F4′, C6—F5′, C6—F6′, C10—F4, C10—F5, C10—F6 (complex **2**) and C2—C3, C17—C16, Dy1—O4 (complex **3**) were restrained to be the same within a standard deviation of 0.001 nm, respectively. Detailed data collection and refinement parameters of complexes **1~3** are summarized in Table 1. Selected important bond lengths and angles are listed in Table 2.

Table 1 Crystallographic data for complexes 1~3

Complex	1	2	3
Empirical formula	$C_{46}H_{46}N_4O_{14}F_{12}Br_2Gd_2$	$C_{46}H_{46}N_4O_{14}F_{12}Br_2Dy_2$	$C_{46}H_{46}F_{12}N_6O_{18}Dy_2$
Formula weight	1 581.17	1 591.67	1 523.89
Crystal system	Triclinic	Triclinic	Triclinic
Space group	$P\bar{1}$	$P\bar{1}$	$P\bar{1}$
a / nm	1.174 5(2)	1.175 72(17)	1.100 29(19)
b / nm	1.185 43(18)	1.184 27(16)	1.169 49(19)
c / nm	1.242 4(2)	1.244 83(18)	1.230 59(10)

Continued Table 1

α / (°)	66.141(17)	66.639(11)	71.707(16)
β / (°)	73.93(2)	73.949(14)	72.531(15)
γ / (°)	65.166(16)	64.922(11)	86.792(19)
V / nm^3	1.423 7(4)	1.428 9(4)	1.432 9(4)
Z	1	1	1
D / (g·cm^{-3})	1.844	1.850	1.776
μ / mm^{-1}	3.815	4.095	2.699
θ range / (°)	1.81~25.01	1.80~25.01	3.04~25.00
F(000)	768	772	748
Crystal size / mm	0.20×0.19×0.04	0.18×0.17×0.05	0.20×0.18×0.06
Reflection collected	14 845	11 881	13 042
Unique reflection	5 003	5 003	4 944
R_{int}	0.031 8	0.032 2	0.058 0
GOF (F^2)	1.069	1.035	1.077
R_1 [$I>2\sigma(I)$]	0.027 3	0.027 7	0.062 9
wR_2 [$I>2\sigma(I)$]	0.067 9	0.061 3	0.143 7
R_1 (all data)	0.030 3	0.031 2	0.087 5
wR_2 (all data)	0.068 9	0.062 5	0.162 9

Table 2 Selected bond lengths (nm) and angles (°) for complexes 1~3

1					
Gd1—O1	0.225 8(3)	Gd1—O7	0.232 9(3)	N1—C17	0.132 9(5)
Gd1—O2	0.230 8(3)	Gd1—O7#1	0.228 2(3)	N1—C18	0.150 5(5)
Gd1—O3	0.227 4(3)	O5—N1	0.130 5(4)	N2—C17	0.138 0(5)
Gd1—O4	0.228 5(3)	O6—N2	0.127 2(5)	N2—C21	0.150 0(6)
Gd1—O5	0.224 4(3)	O7—C11	0.134 1(5)		
O1—Gd1—O2	75.06(11)	O5—N1—C18	120.2(3)	O5—Gd1—O2	79.48(11)
O3—Gd1—O4	76.63(11)	O6—N2—C17	125.3(4)	O5—Gd1—O3	82.04(10)
O5—Gd1—O7	75.32(10)	O6—N2—C21	122.7(4)	O5—Gd1—O4	155.05(11)
O5—N1—C17	126.5(4)	O5—Gd1—O1	113.46(11)		
2					
Dy1—O1	0.228 8(3)	Dy1—O5#2	0.234 2(3)	N1—C19	0.150 2(4)
Dy1—O2	0.230 0(3)	Dy1—O6#2	0.227 1(2)	N2—C17	0.137 3(5)
Dy1—O3	0.228 0(3)	O6—N1	0.129 9(4)	N2—C18	0.149 3(5)
Dy1—O4	0.232 0(3)	O7—N2	0.127 4(4)	O5—C11	0.135 1(4)
Dy1—O5	0.230 0(2)	N1—C17	0.132 3(5)		
O1—Dy1—O2	76.06(9)	O6—N1—C17	127.1(3)	O5—Dy1—O2	82.76(9)
O6#1—Dy1—O5	106.82(9)	O6—N1—C19	120.3(3)	O3—Dy1—O5	117.45(9)
C11—O5—Dy1	127.3(2)	O7—N2—C17	125.5(3)	O5—Dy1—O4	159.78(9)
C11—O5—Dy1#2	120.6(2)	O7—N2—C18	122.4(3)		
3					
Dy1—O1	0.227 5(7)	Dy1—O7	0.233 0(6)	O2—N1	0.127 4(11)
Dy1—O3	0.227 1(8)	Dy1—O7#3	0.234 0(6)	N2—C4	0.148 8(14)
Dy1—O4	0.229 1(6)	O7—Dy1#3	0.234 0(6)	N2—C7	0.132 7(12)

Continued Table 2

Dy1—O5	0.224 5(8)	Dy1—Dy1#3	0.386 27(11)	O7—C13	0.133 5(12)
Dy1—O6	0.238 5(16)	O1—N2	0.129 5(10)		
O5—Dy1—O3	148.2(3)	O3—Dy1—O1	85.2(3)	O5—Dy1—O7	119.5(3)
O5—Dy1—O6	68.1(5)	O6—Dy1—O1	161.0(4)	O2—N1—C7	125.5(10)
O3—Dy1—O6	92.2(5)	O5—Dy1—O4	76.0(3)	O1—N2—C7	125.2(8)
O5—Dy1—O1	105.2(3)	O5—Dy1—O7#3	80.3(3)		

Symmetry codes: #1: $-x$, $-y+1$, $-z+1$ for **1**; #2: $-x+2$, $-y+1$, $-z$ for **2**; #3: $-x+1$, $-y+1$, $-z+1$ for **3**.

CCDC: 1981623, **1**; 1981622, **2**; 2021836, **3**.

2 Results and discussion

2.1 Description of the crystal structures

X-ray single-crystal diffraction analyses confirmed that the structures of all the three complexes are similar and crystallize in the triclinic space group $P\bar{1}$, and that the same radicals were applied to complexes **1** and **2**. Therefore, only the crystal structures of complexes **2** and **3** are described in detail as the representative samples. As shown in Fig. 1 and 2, complexes **2** and **3** are dinuclear complexes comprising of two [Dy(tfac)$_2$(NIT-5Br-2PhO)]/[Dy(tfac)$_2$(NIT-5NO$_2$-2PhO)] units bridged through two phenoxo groups. For both complexes, seven-coordinated Dy (Ⅲ) ions are surrounded by four oxygen atoms from two chelating ligand of tfac anions, one oxygen atom from the N—O group and two phenoxo - O anions of two nitronyl nitroxide radicals (Fig. 3 and 4). And the phenoxo - O atoms also link to

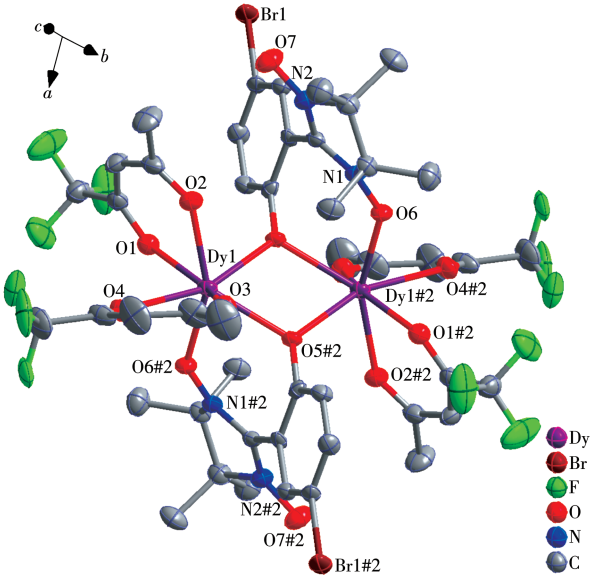

All hydrogen atoms are omitted for clarity; Symmetry code: #2: $-x+2$, $-y+1$, $-z$

Fig.1 Crystal structure of complex **2** with thermal ellipsoids at 50% probability level

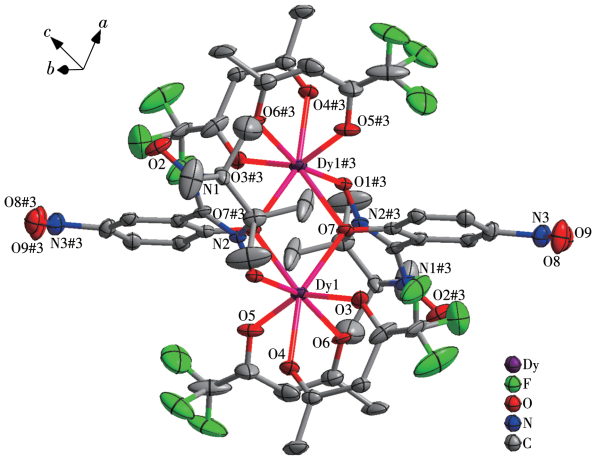

All hydrogen atoms are omitted for clarity; Symmetry code: #3: $-x+1$, $-y+1$, $-z+1$

Fig.2 Crystal structure of complex **3** with thermal ellipsoids at 50% probability level

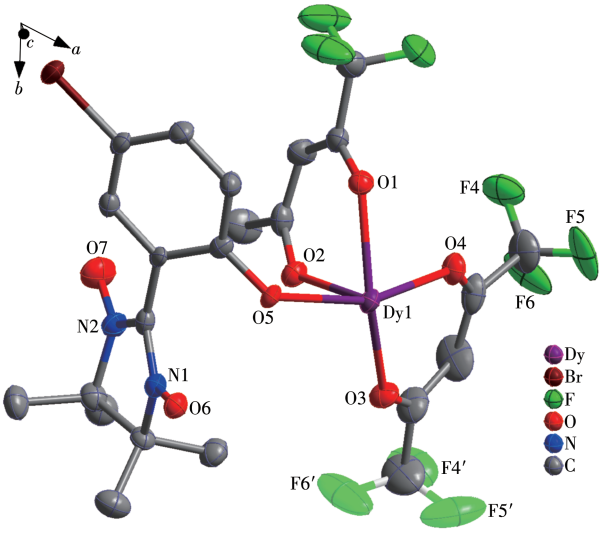

All hydrogen atoms are omitted for clarity

Fig.3 Asymmetric unit of complex **2** with thermal ellipsoids at 50% probability level

the other Dy(Ⅲ) ion forming one binuclear complex. The coordinated N—O bond length of the radicals are 0.129 9(4) and 0.128 8(10) nm, while the uncoordinated ones are 0.127 3(4) and 0.128 0(12) nm, for **2** and **3**, respectively, indicating the existence of the nitronyl nitroxide radical on complexes. The Dy—$O_{phenoxo}$ distances are 0.230 0(2) and 0.234 2(3) nm for complex **2**, 0.232 9(6) and 0.234 1(6) nm for complex **3**; the Dy—$O_{radical}$ distances are 0.227 0(2) nm for **2** and 0.227 9(7) nm for **3**; the Dy—O_{tfac} bond lengths are in a range of 0.228 0(3)~0.231 9(3) nm and 0.224 8(9)~0.229 0(6) nm for complexes **2** and **3**, respectively; the Dy—Dy distances in Dy_2O_2 cores are 0.384 80(9) nm for **2** and 0.386 25(11) nm for **3**; the Dy—O—Dy bridge bond angle are 111.98(9)° and 111.6(3)° for complexes **2** and **3**, respectively, which are slightly changed but comparable to those of the reported complexes assembled by Dy(Ⅲ) ions with phenoxo-O anions nitronyl nitroxide radicals[45-46]. For example, apparently the Dy—$O_{radical}$ bond lengthes in complexes **2** and **3** are slightly shorter than the corresponding Dy—$O_{radical}$ bond length (0.232 0(3) nm) in $[Dy_2(acac)_4(NITPhO)_2]$ and longer than the corresponding Dy—$O_{radical}$ bond length (0.221 9(4) nm) in $[Dy_2(hfac)_4(NIT5BrPhO)_2]$; the Dy—O—Dy bridge bond angles of complexes **2** and **3** are smaller than the bond angle of 112.88(12)° in $[Dy_2(acac)_4(NITPhO)_2]$[45] but bigger than the bond angle of 110.64(17)° in $[Dy_2(hfac)_4(NIT5BrPhO)_2]$[46]. The analysis of complexes **2~3** and $[Dy_2(acac)_4(NITPhO)_2]$, $[Dy_2(hfac)_4(NIT5BrPhO)_2]$ as reported in the previous literatures shows that maybe the distinct differences of them are the number of F-substituent on the β-diketonate coligands and the symmetry of the β-diketonate coligands. This will result in a different electro-withdrawing effect induced by F atoms, and the strength of the local ligand field of the Dy(Ⅲ) ion in complexes **2** and **3** will be weaker than the Dy(Ⅲ) in $[Dy_2(acac)_4(NITPhO)_2]$ but stronger than the Dy(Ⅲ) in $[Dy_2(hfac)_4(NIT5BrPhO)_2]$. Furthermore, the data also strongly prove that the modification of coligand and functionalized radical ligand can affect the paramters of crystal structure. The polyhedral shape of the central Ln(Ⅲ) ions has been analyzed by continuous shape measures[47] employing the SHAPE program. The results presented in Table 3 reveal that the capped octahedron is the best description for the geometry of LnO_7 in these complexes, and the configuration of DyO_7 in complex **2** is shown in Fig.5. The packing diagrams of complexes **2** and **3** are shown in Fig.S2 and S3 (Supporting information), respectively. The shortest Dy…Dy distance between the adjacent molecules are 0.100 81 and 0.759 6 nm, and the shortest contact between the uncoordinated NO groups is 0.396 6 and 0.753 5 nm for **2** and **3**, respectively. The large separation implies the complexes molecules are well isolated in the solid state, but the possible weak intermolecular interaction is not ruled out.

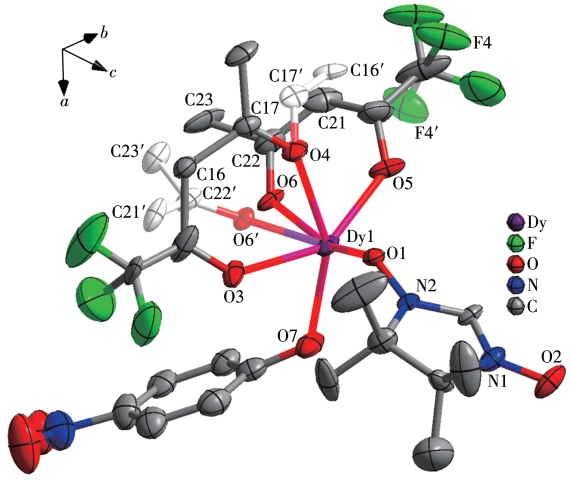

All hydrogen atoms are omitted for clarity

Fig.4 Asymmetric unit of complex **3** with thermal ellipsoids at 50% probability level

Table 3 SHAPE analysis for complexes 1~3

Complex	PBPY-7(D_{5h})	COC-7(C_{3v})	CTPR-7(C_{2v})	JPBPY-7(D_{5h})	JETPY-7(C_{3v})
1	7.054	0.414	1.269	10.455	18.847
2	7.094	0.456	1.246	10.540	18.725
3	6.516	0.496	1.204	10.004	18.606

PBPY-7: pentagonal bipyramid; COC-7: capped octahedron; CTPR-7: capped trigonal prism; JPBPY-7: Johnson pentagonal bipyramid J13; JETPY-7: Johnson elongated triangular pyramid J7.

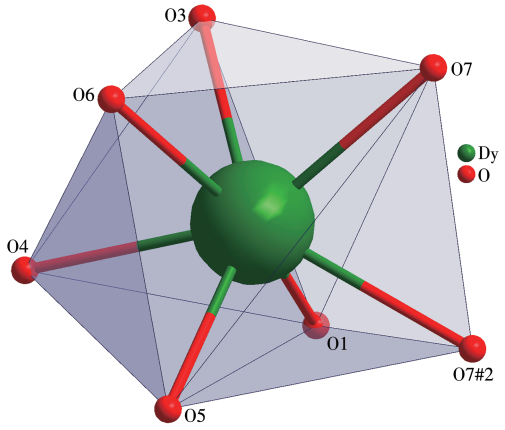

Symmetry code: #2: $-x+2, -y+1, -z$

Fig.5 View of coordination sphere of Dy(Ⅲ) in complex **2**

2.2 Magnetic properties

The magnetic properties of complexes **1~3** have been investigated in a temperature range of 2.0~300 K under the applied magnetic field of 1 kOe. Their magnetic behaviors ($\chi_M T$ vs T curves) are shown in Fig.6~8.

For complex **1**, at the highest temperature 300 K, the value of $\chi_M T$ was 16.94 $cm^3 \cdot K \cdot mol^{-1}$, which was close to the expected value 16.5 $cm^3 \cdot K \cdot mol^{-1}$ for four uncoupled spin carriers: two Gd(Ⅲ) ions ($^8S_{7/2}$, S=7/2, L=0, g=2, $\chi_M T$=7.88 $cm^3 \cdot K \cdot mol^{-1}$) and two organic radical (S=1/2). On lowering temperature, the $\chi_M T$ value gradually decreased to reach a minimum of 11.67 $cm^3 \cdot K \cdot mol^{-1}$ at 2 K (Fig.6). The overall magnetic behavior indicates the antiferromagnetic interactions dominate in this complex. According to the crystal structure, the main existing magnetic interactions include: (1) the interaction between Gd(Ⅲ) ion and coordinated radical

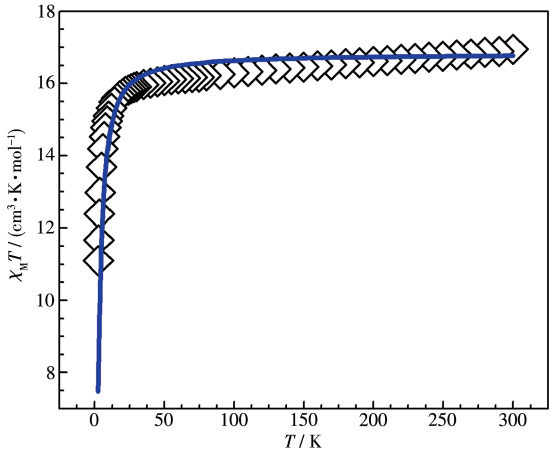

Solid line represents the calculated behavior

Fig.6 $\chi_M T$ vs T plot for complex **1**

(J_1); (2) the magnetic coupling interaction between Gd(Ⅲ)-Gd(Ⅲ) by the phenolate bridges (J_2). For the present system, the Kambe vector-coupling method cannot be used to calculate the variable-temperature susceptibility data. So, the magnetism package MAGPACK was employed to simulate the magnetic susceptibility data through the spin Hamiltonian theoretical expression $\hat{H} = -2J_1(\hat{S}_{rad1}\hat{S}_{Gd1} + \hat{S}_{rad2}\hat{S}_{Gd2}) - 2J_2\hat{S}_{Gd1}\hat{S}_{Gd2}$, leading to the optimal fitting parameters: g=2.02, J_1=0.85 cm^{-1}, J_2=−0.16 cm^{-1}. Furthermore, the positive J_1 value proves that there is weak ferromagnetic interactions between Gd(Ⅲ) ion and the coordinated NO group. This ferromagnetic interaction may be due to electron transfer involving the magnetic orbital of the free radical (π^*) and the vacant orbitals of the Gd(Ⅲ) ion (5*d* or 6*s*) that stabilize the higher multiplicity ground spin state following Hund′s rule[48-49]. Meanwhile, the negative J_2 value reflects antiferromagnetic interactions between two Gd(Ⅲ) ions by the phenoxo-O anion bridges, which is in line with those similar phenoxo-linked Ln complexes in literature[45].

For complexes **2** and **3**, the $\chi_M T$ value were 28.70 and 29.51 $cm^3 \cdot K \cdot mol^{-1}$, respectively, which were all close to the expected value of 29.09 $cm^3 \cdot K \cdot mol^{-1}$ for two uncoupled Dy(Ⅲ) ions ($^6H_{15/2}$, $\chi_M T$=14.17 $cm^3 \cdot K \cdot mol^{-1}$) and two uncorrelated radical spins (S=1/2), but slightly different from the expected value. Specifically, the $\chi_M T$ value of complex **2** was lower than the expected value while the one of complex **3** was higher than it. Upon cooling, the $\chi_M T$ value of complexes **2** and **3** decreased gradually and reached minimum of 17.01 and 14.95 $cm^3 \cdot K \cdot mol^{-1}$ at 2 K, respectively (Fig.7 and 8). Their magnetic behaviors can be mainly ascribed to the progressive depopulation of the levels of multiplet with J=15/2 of the Dy(Ⅲ) ions[50]. The Dy(Ⅲ) ion interacted with the coordinated NO group and the indirect interaction mediated through the phenolate bridges of Dy(Ⅲ) ions. The ferromagnetic behavior of the system can be judged according to this behavior. At present, it is hard to quantify the different contributions, but the Dy(Ⅲ) stark sublevel may be dominant.

To explore the spin dynamics, the magnetic measurements of alternating current (ac) were carried out

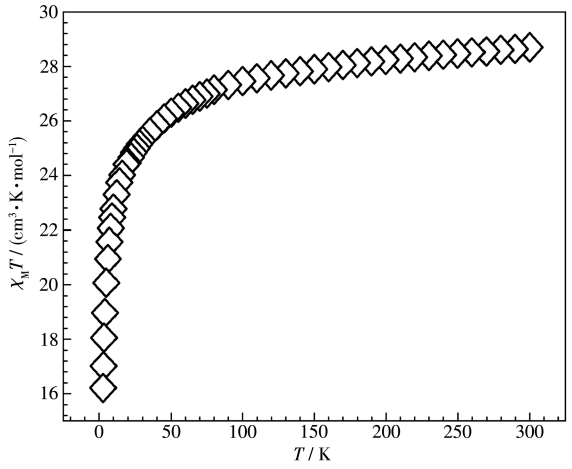

Fig.7 $\chi_M T$ vs T plot for complex **2**

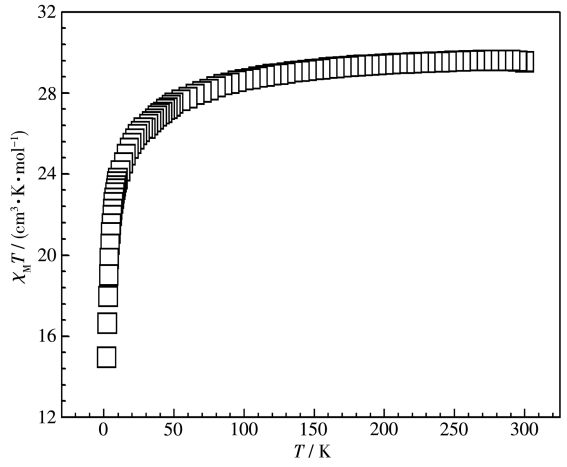

Fig.8 $\chi_M T$ vs T plot for complex **3**

for complex **3** under an ac field of 3 Oe based on a zero direct-current (dc) field (Fig.9). There were no non-zero out-of-phase (χ_M'') signals, which may be ascribed to quantum tunneling of the magnetization (QTM). To suppress QTM and remove the degeneracy of the levels on opposite sides of the anisotropy barrier further, ac magnetic susceptibilities were measured using a 3 kOe dc field (Fig.S4). But regrettably, non-zero χ_M'' signals still are not observed, suggesting that the quantum tunneling effect at zero-field is negligible for complex **3**.

It is interesting to compare complex **3** with the previously reported complex $[Dy_2(hfac)_4(NITPhO)_2]$ [46], for the two complexes owning similar structure but different magnetic behavior. Obviously, after replacing the β-diketonate coligand hfac with the tfac, no distinct deviations have been found in two complexes′ crystal structure features, but their magnetic properties are slightly different. The structure analysing for the two

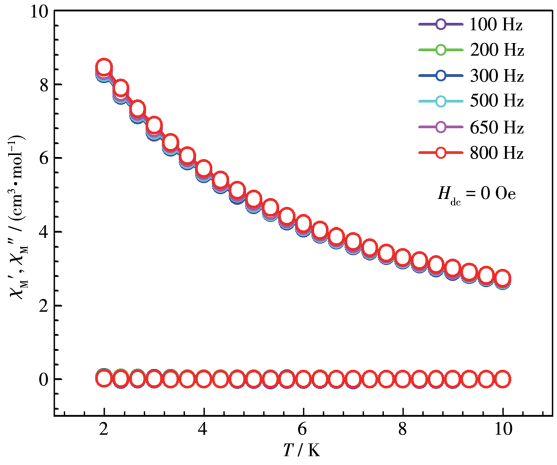

Fig.9 Temperature dependence of in-phase (χ_M') and out-of-phase (χ_M'') components of ac susceptibility for complex **3** in zero dc field with an oscillating of 3 Oe

complexes show that the distinct difference is the number of F-substituent on the directly coordinated β-diketonate coligand which will result in different strengths of the local ligand field of Dy(Ⅲ) ion for two complexes. In addition, the electro-withdrawing effect induced by the NO_2 group of the radical also will have an effect on the strength of the local ligand field of metal ion. So, the different local ligand-fields of the Ln(Ⅲ) ions lead to different magnetic dynamic behaviors of the two complexes.

3 Conclusions

In conclusion, three new lanthanide-radical complexes have been successfully achieved. These 2*p*-4*f* complexes feature a tetra-spin system in which the radical ligands act as a bridge linking two Ln(Ⅲ) ions via the oxygen atoms of the phenolate groups. Furthermore, the temperature dependencies of magnetic susceptibilities for the three complexes were studied. The magnetic coupling between the radical and the Gd(Ⅲ) is ferromagnetic while magnetic interaction between two Gd(Ⅲ) ions through the phenolate groups is antiferromagnetic. No slow magnetic relaxation behavior was observed for complex **3**.

Acknowledgements: This work is supported by the Natural Science Foundation of Anhui Universities (Grant No. KJ2017A571), the Natural Science Foundation of Bengbu University (Grant No. 2017ZR01zd), the Industry-University-

Research Project (Optimization of Molding Process Parameters for Precision Plastic Parts) and the College Students Innovation and Entrepreneurship Project (Grant No.201811305146).

Supporting information is available at http://www.wjhxxb.cn

References:

[1] Poneti G, Bernot K, Bogani L, Caneschi A,Sessoli R, Wernsdorfer W, Gatteschi D. *Chem. Commun.*, **2007**,**18**:1807-1809

[2] Gatteschi D, Sessoli R. *Angew. Chem. Int. Ed.*, **2003**,**42**:268-297

[3] Sessoli R, Powell A K. *Coord. Chem. Rev.*, **2009**,**253**:2328-2341

[4] Luzon J, Sessoli R. *Dalton. Trans.*, **2012**,**41**:13556-13567

[5] Chen Y C, Liu J L, Ungur L, Liu J, Li Q W, Wang L F, Ni Z P, Chibotaru L F, Chen X M, Tong M L. *J. Am. Chem. Soc.*, **2016**,**138**:2829-2837

[6] Woodruff D N, Winpenny R E P, Layfield R A. *Chem. Rev.*, **2013**, **113**:5110-5148

[7] Habib F, Murugesu M. *Chem. Soc. Rev.*, **2013**,**42**:3278-3288

[8] 胡鹏, 吴燕妮, 黄期晓, 连思绵, 付兴慧, 何高鹏, 陈侠敏. 无机化学学报, **2016**,**32**(2):297-304
HU P, WU Y N, HUANG Q X, LIAN S M, FU X H, HE G P, CHEN X M. *Chinese J. Inorg. Chem.*, **2016**,**32**(2):297-304

[9] 胡鹏, 高媛媛, 肖凤仪, 邓肖娟, 黄国洪, 张淼, 苏芬, 王莉娜. 无机化学学报, **2017**,**33**(1):33-40
HU P, GAO Y Y, XIAO F Y, DENG X J, HUANG G H, ZHANG M, SU F, WANG L N. *Chinese J. Inorg. Chem.*, **2017**,**33**(1):33-40

[10]Booth C H, Walter M D, Kazhdan D, Hu Y J, Lukens W W, Bauer E D, Maron L, Eisenstein O, Andersen R A. *J. Am. Chem. Soc.*, **2009**, **131**:6480-6491

[11]Caneschi A, Dei A, Gatteschi D, Sorace L, Vostrikova K. *Angew. Chem. Int. Ed.*, **2000**,**39**:246-248

[12]Gurek A G, Basova T, Luneau D, Lebrun C, Kol′tsov E, Hassan A K, Ahsen V. *Inorg. Chem.*, **2006**,**45**(4):1667-1676

[13]Kanetomo T, Ishida T. *Chem. Commun.*, **2014**,**50**(19):2529-2531

[14]Trifonov A A, Gudilenkov I D, Larionova J, Luna C, Fukin G K, Cherkasov A V, Poddel′sky A I, Druzhkov N O. *Organometallics*, **2009**,**28**(23):6707-6713

[15]Ganivet C R, Ballesteros B, de la Torre G, Clemente-Juan J M, Coronado E, Torres T. *Chem. Eur. J.*, **2013**,**19**(4):1457-1465

[16]Bernot K, Pointillart F, Rosa P, EtienneM, Sessoli R, Gatteschi D. *Chem. Commun.*, **2010**,**46**(35):6458-6460

[17]Tian L, Sun Y Q, Na B, Cheng P. *Eur. J. Inorg. Chem.*, **2013**(24): 4329-4335

[18]Li X, Li T, Tian L, Liu Z Y, Wang X G. *RSC Adv.*, **2015**,**5**(91):74864-74873

[19]Li H D, Xie J, Xi L, Zhai L J, Niu Y L. *Inorg. Chim. Acta*, **2020**,**499**: 119188

[20]Demir S, Gonzalez M I, Darago L E, Evans W J, Long J R. *Nat. Commun.*, **2017**,**8**:2144

[21]Liu R N, Liu L, Fang D, Xu J, Zhao S P, Xu W L. *Z. Anorg. Allg. Chem.*, **2015**,**641**(3/4):728-731

[22]Reis S G, Briganti M, Soriano S, Guedes G P, Calancea S, Tiseanu C, Novak M A, del Aguila-Sanchez M A, Totti F, Lopez-Ortiz F, Andruh M, Vaz M G F. *Inorg. Chem.*, **2016**,**55**(22):11676-11684

[23]Demir S, Nippe M, Gonzalez M I, Long J R. *Chem. Sci.*, **2014**,**5**(12): 4701-4711

[24]Demir S, Zadrozny J M, Nippe M, Long J R. *J. Am. Chem. Soc.*, **2012**, **134**(45):18546-18549

[25]Rinehart J D, Fang M, Evans W J, Long J R. *Nat. Chem.*, **2011**,**3**(7): 538-542

[26]Meihaus K R, Corbey J F, Fang M, Ziller J W, Long J R, Evans W J. *Inorg. Chem.*, **2014**,**53**(6):3099-3107

[27]Pointillart F, Le Gal Y, Golhen S, Cador O, Ouahab L. *Chem. Commun.*, **2009**(25):3777-3779

[28]Dei A, Gatteschi D, Massa C A, Pardi L A, Poussereau S, Sorace L. *Chem. Eur. J.*, **2000**,**6**:4580-4586

[29]Pointillart F, Le Guennic B, Golhen S, Cador O, Ouahab L. *Chem. Commun.*, **2013**,**49**:11632-11634

[30]Reis S G, Briganti M, Martins D O T A, Akpinar H, Calancea S, Guedes G P, Soriano S, Andruh M, Cassaro R A A, Lahti P M, Totti F, Vaz M G F. *Dalton Trans.*, **2016**,**45**(7):2936-2944

[31]Li H D, Sun Z, Sun J, Xi L, Guo J N, Sun G F, Xie J, Ma Y, Li L C. *J. Mater. Chem. C*, **2018**,**6**(8):2060-2068

[32]Chen P Y, Wu M Z, Li T, Shi X J, Tian L, Liu Z Y. *Inorg. Chem.*, **2018**,**57**(20):12466-12470

[33]Xi L, Sun J, Li H D, Han J, Huang X H, Li L C. *Cryst. Growth Des.*, **2020**,**20**(6):3785-3794

[34]Raebiger J W, Miller J S. *Inorg. Chem.*, **2002**,**41**(12):3308-3312

[35]Romanov V E, Bagryanskaya I Y, Gorbunov D E, Gritsan N P, Zaytseva E V, Luneau D, Tretyakov E V. *Crystals*, **2018**,**8**(9):334

[36]Tian H X, Liu R N, Wang X L, Yang P P, Li Z X, Li L C, Liao D Z. *Eur. J. Inorg. Chem.*, **2009**:4498-4502

[37]Pointillart F, Bernot K, Poneti G, Sessoli R. *Inorg. Chem.*, **2012**,**51** (22):12218-12229

[38]Katagiri S, Tsukahara Y, Hasegawa Y, Wada Y. *Bull. Chem. Soc. Jpn.*, **2007**,**80**:1492-1503

[39]Das B, Venkateswarlu K, Majhi A, Siddaiah V, Reddy K R. *J. Mol. Catal. A*, **2007**,**267**:30-33

[40]Ullman E F, Call L, Osiecki J H. *J. Org. Chem.*, **1970**,**35**:3623

[41]Davis M S, Morokuma K, Kreilick R W. *J. Am. Chem. Soc.*, **1972**,**94**: 5588

[42]Sheldrick G M. *SHELXLS*-97, *Program for the Solution of Crystal Structures*, University of Göttingen, Germany, **1997**.

[43]Sheldrick G M. *SHELXL*-97, *Program for the Refinement of Crystal Structures*, University of Göttingen, Germany, **1997**.

[44]Zhang J, Ma X F, Xuan X P. *Chin. J. Struct. Chem.*, **2020**,**39**(4):698-708

[45]Mei X L, Wang X F, Wang J J, Ma Y, Liao D Z. *New J. Chem.*, **2013**, **37**:3620-3626

[46]Liu R N, Zhang C M, Li L C, Liao D Z, Sutter J P. *Dalton Trans.*, **2012**,**41**(39):12139-12144

[47]*SHAPE Ver.* 2.1, University of Barcelona and The Hebrew University of Jerusalem, Barcelona, **2005**.

[48]Benelli C, Caneschi A, Gatteschi D, Guillou O, Pardi L. *Inorg. Chem.*, **1990**,**29**:1750-1755

[49]Andruh M, Ramade I, Godjovi E, Guillou O, Kahn O, Trombe J C. *J. Am. Chem. Soc.*, **1993**,**115**:1822-1829

[50]Datcu A, Roques N, Jubera V, Maspoch D, Fontrodona X, Wurst K, Imaz I, Mouchaham G, Sutter J P, Rovira C, Veciana J. *Chem. Eur. J.*, **2012**,**18**(1):152-162